Supplementary figure 1

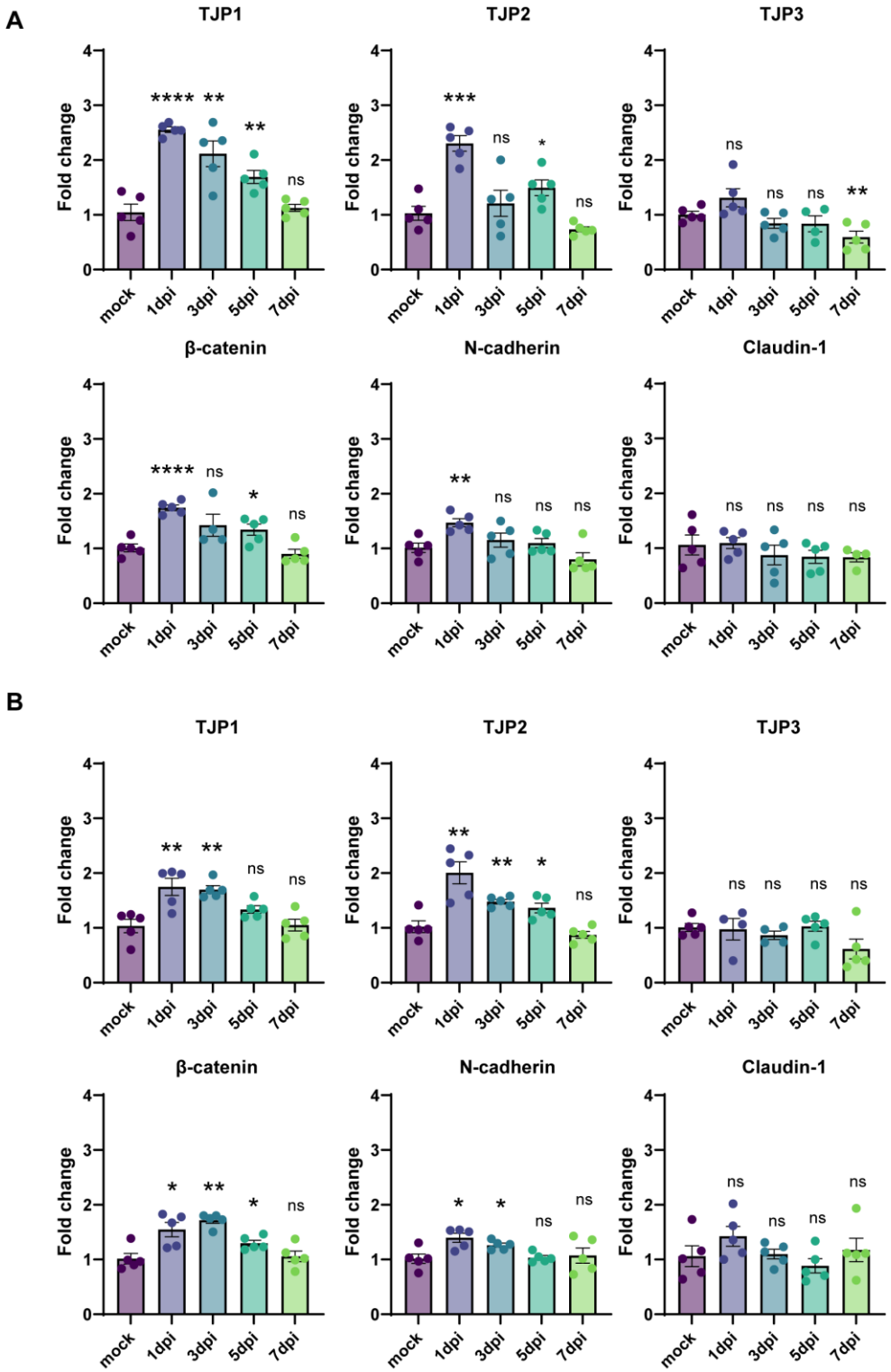

SF 1. Expression of tight junction proteins and adhesion molecules in brain tissue following DENV infection. Expression levels of TJP1, TJP2, TJP3, Claudin-1, β-catenin and N-cadherin in brain tissue of DENV i.v. infected mice (A) or i.p. infected mice (B) compared to mock-infected controls, respectively. Data are presented as fold change relative to mock group. * $p < 0.05$, ** $p < 0.01$. ***$p < 0.001$. ****$p < 0.0001$. Data are presented as mean ± SEM.

Supplementary figure 2

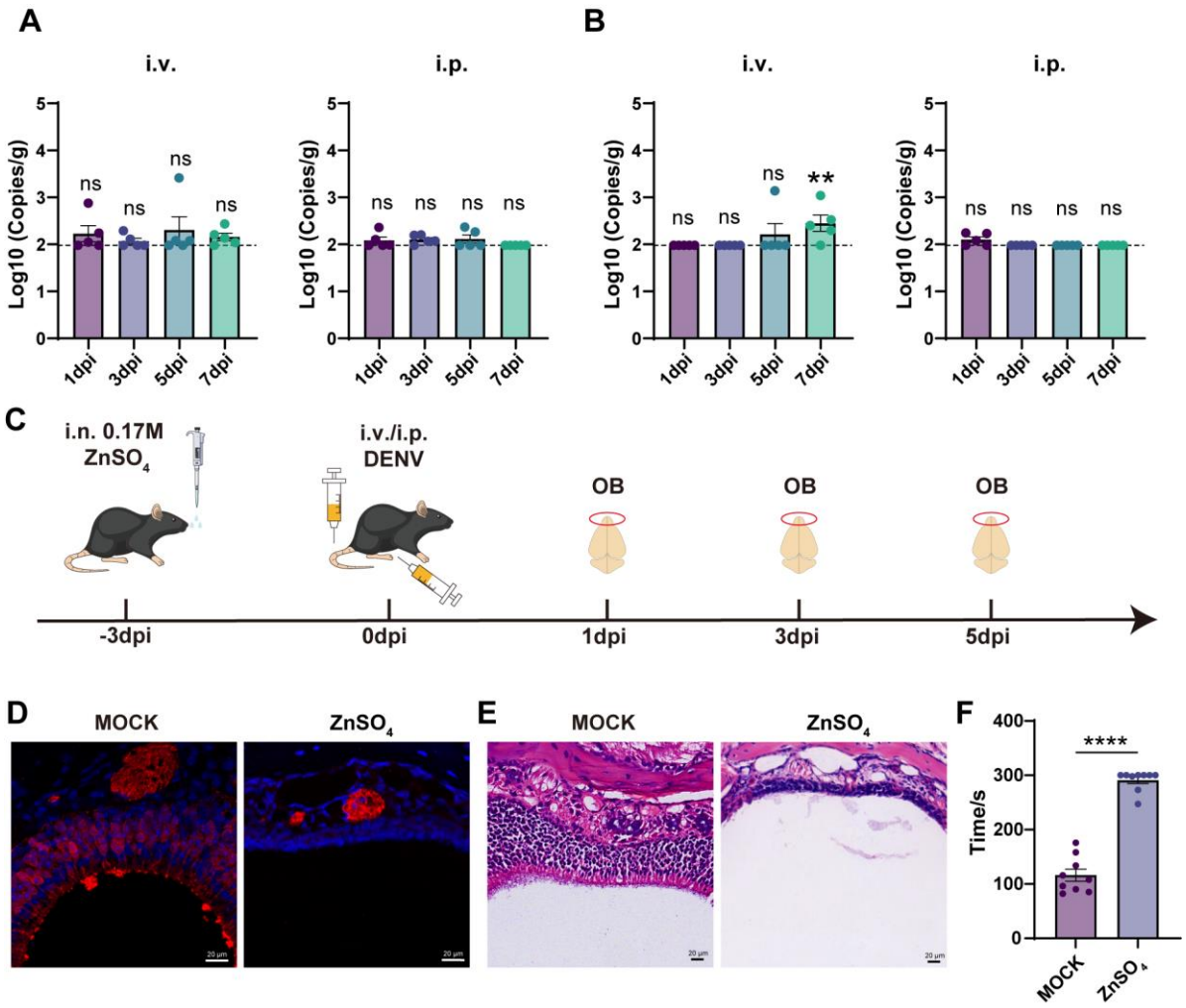

SF 2. Viral load and olfactory changes in mice following DENV infection and $ZnSO_4$ treatment. (A, B) Viral RNA loads in the cortex (A) and hippocampus (B) of mice at 1, 3, 5, and 7 dpi following DENV infection via i.v. or i.p. routes, compared to mock-infected controls (n=5).(C) Schematic of the experimental timeline for $ZnSO_4$ treatment. (D) Representative immunofluorescence images of olfactory mucosa stained for olfactory marker protein (OMP) in mice after intranasal $ZnSO_4$ treatment. Nuclei are counterstained with DAPI (blue). Scale bar = 20 μm. (E) Hematoxylin and eosin (H&E) staining of olfactory mucosa in mice after intranasal treatment with 0.17M $ZnSO_4$. Scale bar = 20 μm. (F) Results of the food buried test showing increased time to locate food in mice after intranasal $ZnSO_4$ treatment, indicating olfactory dysfunction (n=9). ****$p < 0.0001$. Data are presented as mean ± SEM.

Supplementary figure 3

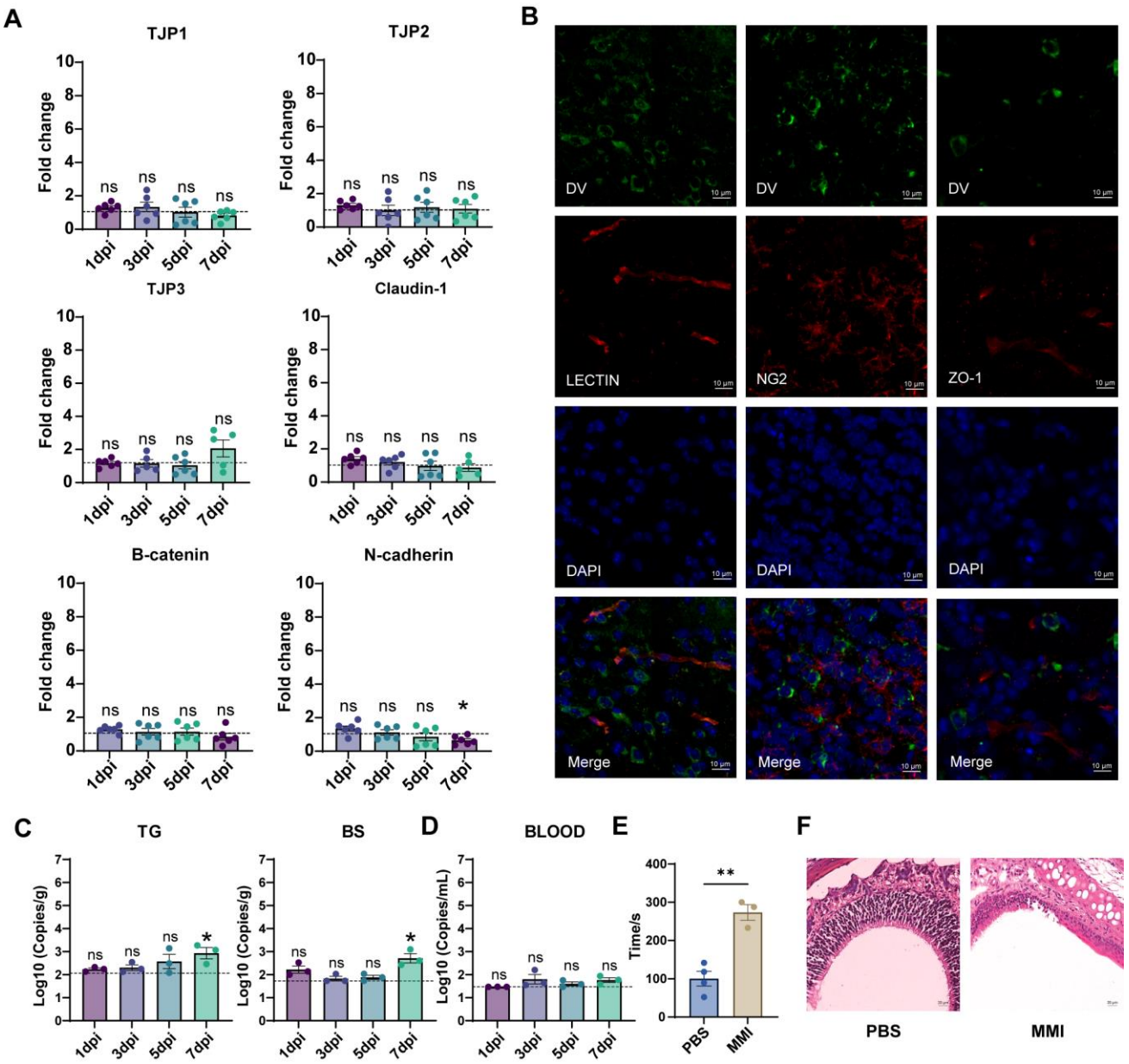

SF 3. Characteristics of BBB integrity and non-olfactory pathways. (A) Expression levels of TJP1, TJP2, TJP3, Claudin1, β-catenin and N-cadherin in brain tissue of DENV i.n. infected mice compared to mock-infected controls. Data are presented as fold change relative to mock group (n=6). (B) Representative immunofluorescence images of brain sections stained with antibodies against lectin, NG2, and ZO-1 in DENV i.n. infected mice. Nuclei are counterstained with DAPI (blue). Scale bar = 10 μm. (C) Viral RNA loads detected in trigeminal ganglia (TG) and brainstem (BS) of mice at 1, 3, 5, and 7dpi. Data are presented as viral RNA copies/g of total RNA (n=3). (D) Viral RNA levels detected in blood samples of mice at 1, 3, 5, and 7dpi. Data are presented as viral RNA copies/mL of blood (n=3). (E) Results of the food buried test showing increased time to locate food in mice after intraperitoneal injection of methimazole (50 mg/kg, n=3-4). (F) H&E staining of olfactory mucosa in mice after intraperitoneal injection of methimazole. Scale bar = 20 μm. *$p < 0.05$, ** $p < 0.01$. Data are presented as mean ± SEM.

Supplementary figure 4

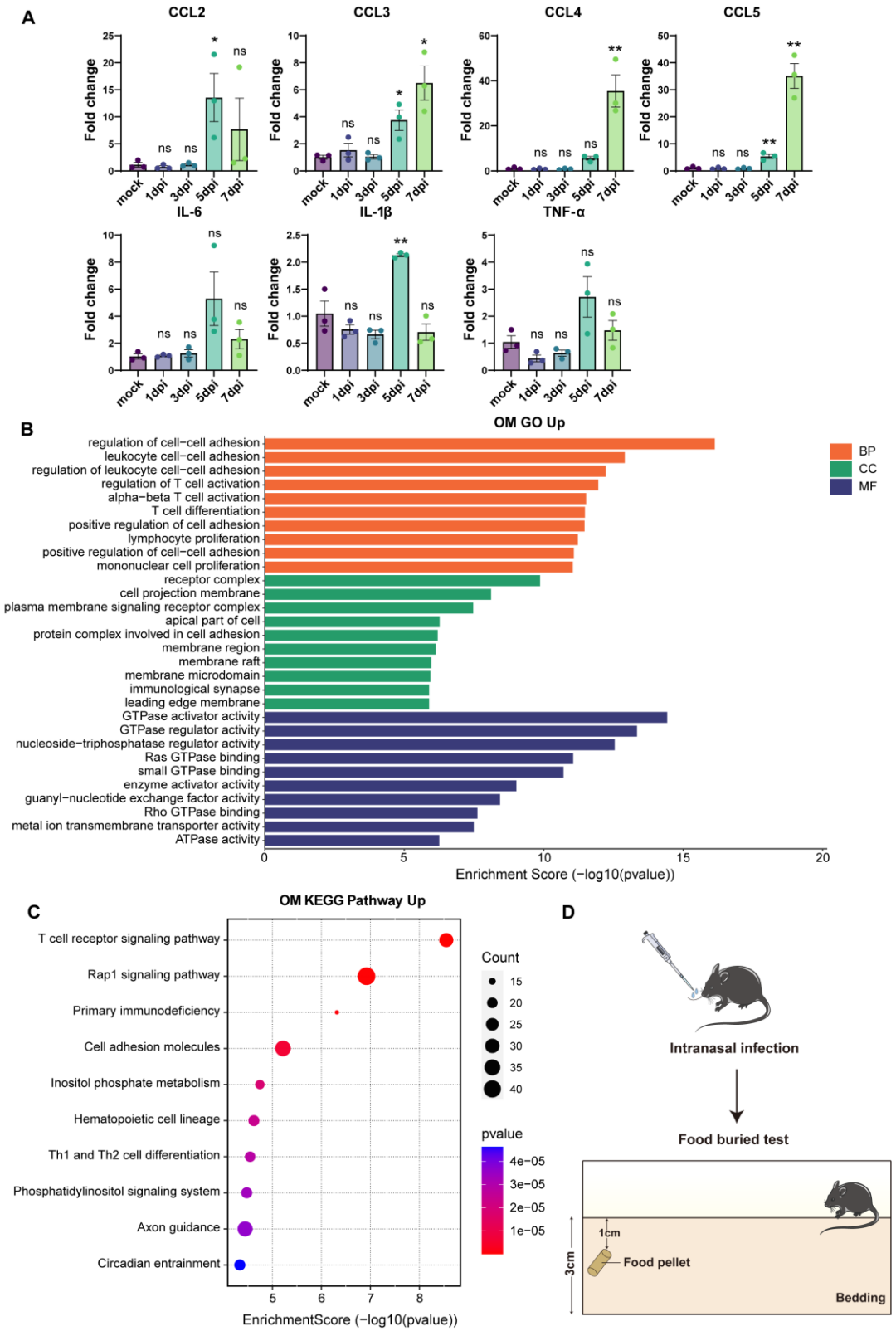

SF 4. Molecular and functional changes in olfactory mucosa following intranasal DENV infection. (A) Expression levels of TJP1, TJP2, TJP3, Claudin1, β-catenin and N-cadherin in olfactory mucosa of DENV i.n. infected mice compared to mock-infected controls. (B) GO enrichment analysis of upregulated genes in olfactory mucosa of DENV i.n. infected mice. (C) KEGG pathway enrichment analysis of upregulated genes in olfactory mucosa of DENV i.n. infected mice. (D) Schematic diagram illustrating the setup and procedure of the food burial test following intranasal infection with DENV. * $p < 0.05$, **$p < 0.01$. Data are presented as mean ± SEM.

Supplementary figure 5

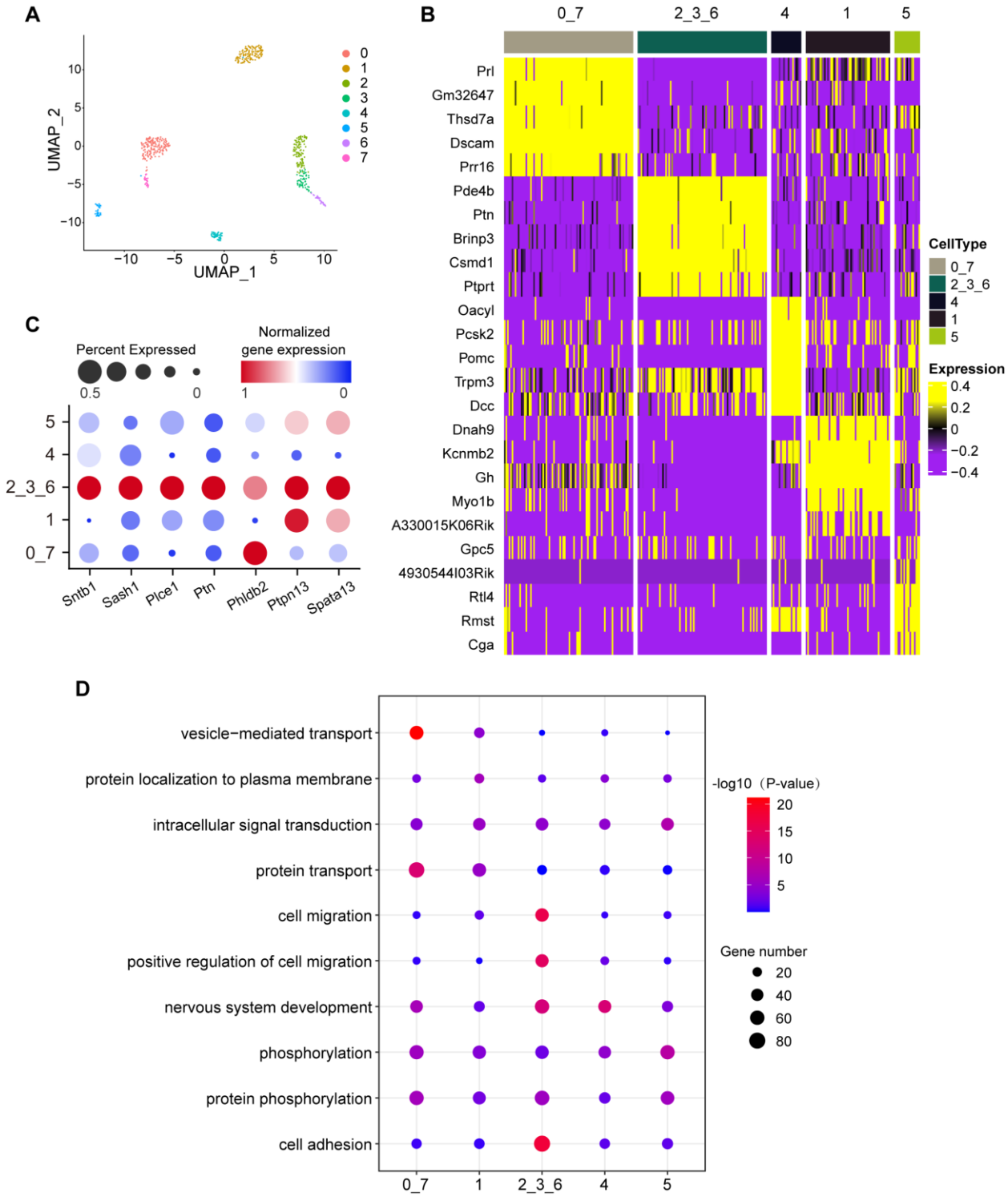

SF 5. Characteristic of OECs in snRNA-seq. (A) UMAP projection of OEG cells, revealing 5 distinct clusters (n = 595 cells). (B) Top 5 differentially expressed genes for each of the 5 OEG clusters. (C) Bubble plot showing the expression levels of OEG marker genes across the 5 cell clusters. (D) GO enrichment analysis of the differentially expressed genes in the 5 OEG clusters.

Supplementary figure 6

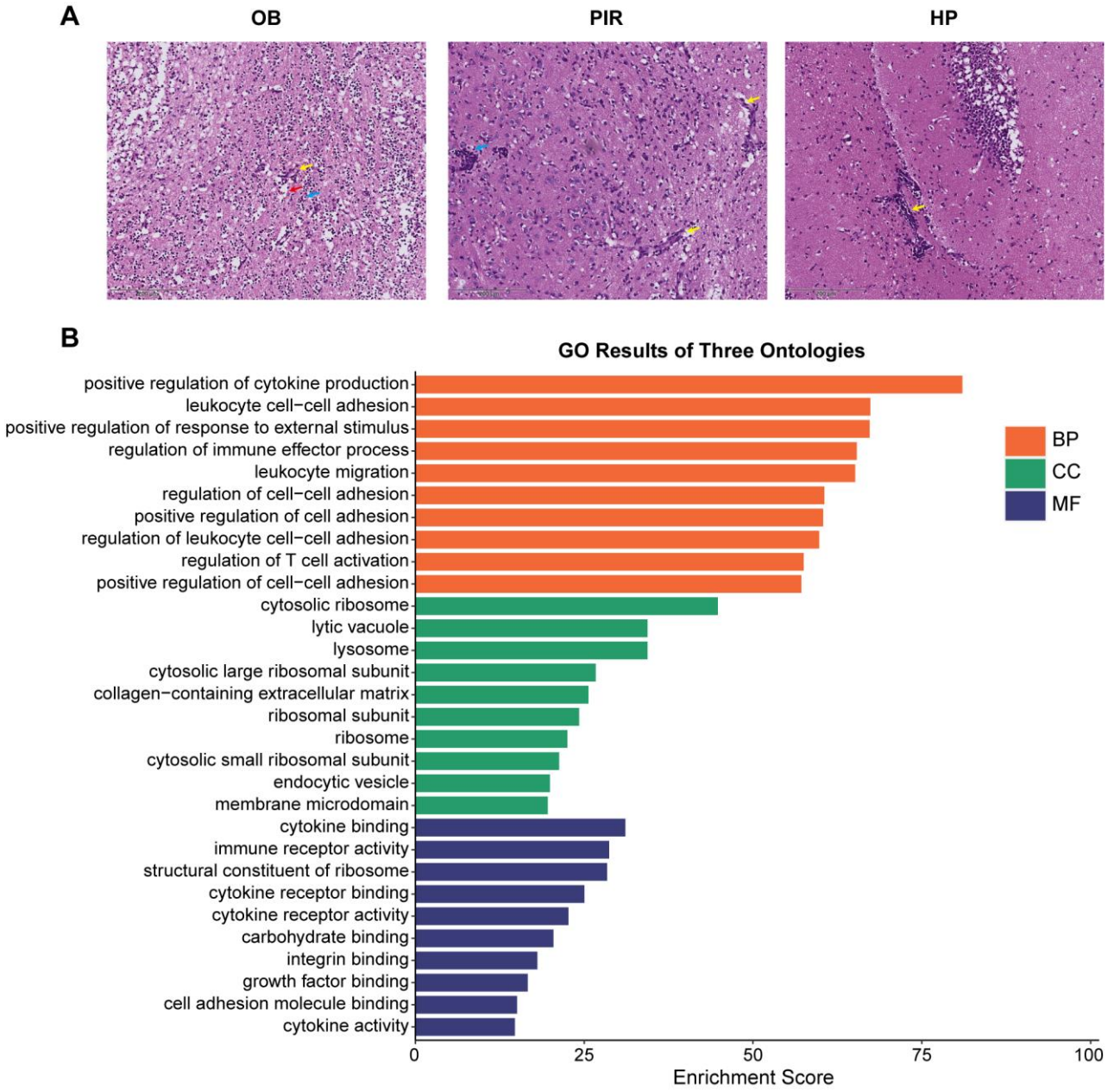

SF 6. Histological and molecular changes in brain regions following intranasal infection. (A) Hematoxylin and eosin (H&E) staining of brain sections from mice after intranasal infection, showing the olfactory bulb (OB), piriform cortex (Pir), and hippocampus (HP). Yellow arrows indicate vascular sleeves, blue arrows indicate immune cell infiltration, and red arrows indicate vacuolization. Scale bar = 200 μm. (B) GO enrichment analysis of upregulated genes in OB.

Supplementary figure 7

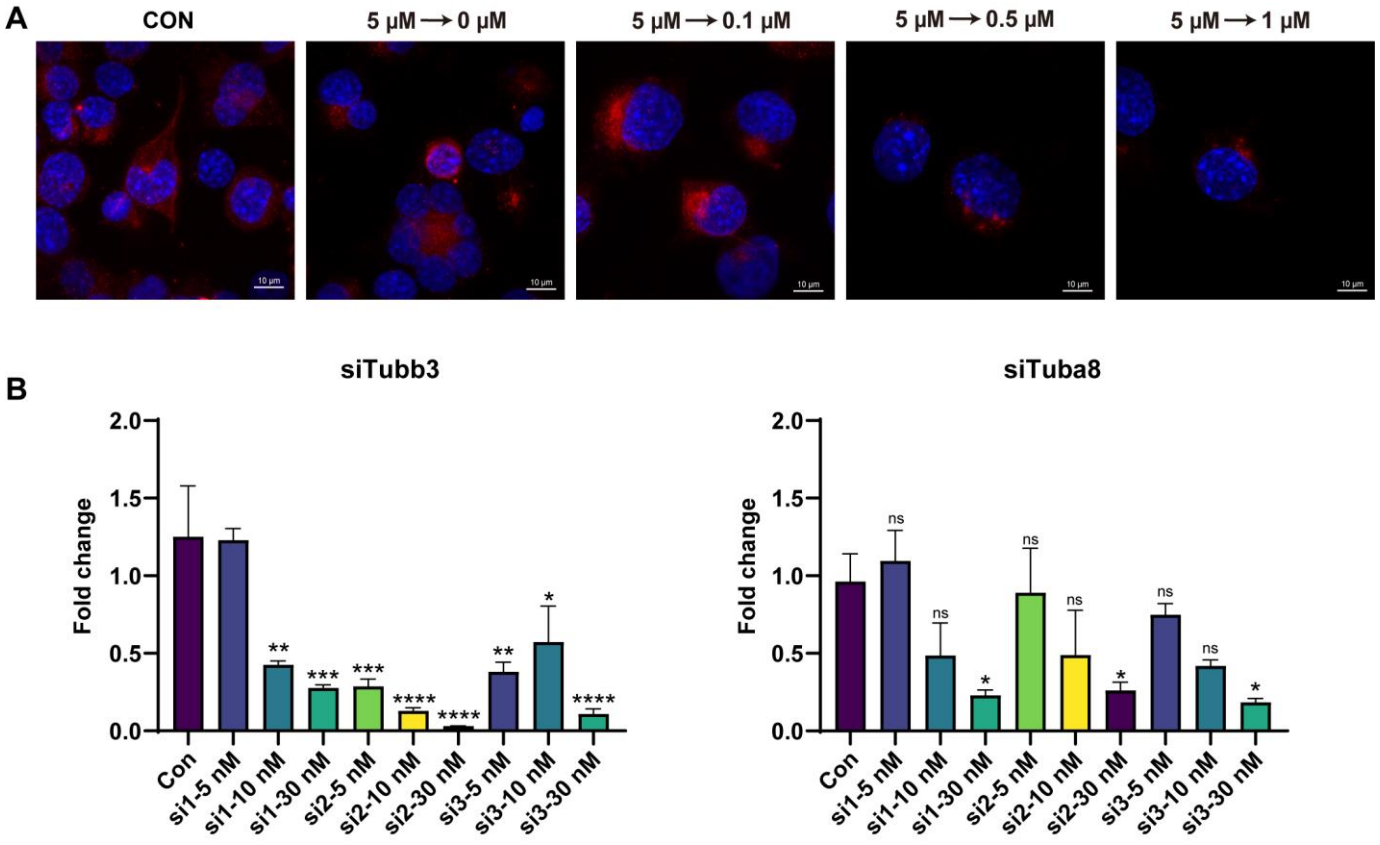

SF 7. Validation of nocodazole treatment and siRNA knockdown efficiency. (A) Neuro-2a cells were pretreated with 5 μM nocodazole for 4 h, washed, and maintained in the indicated concentrations (0–1 μM) for 24 h. Acetylated α-tubulin levels (red) were detected by immunofluorescence. Nuclei are counterstained with DAPI (blue). Scale bar=10 μm. (B) RT-qPCR validation of tubb3 and tuba8 knockdown efficiency in Neuro-2a cells transfected with three independent siRNAs per gene. * $p < 0.05$, ** $p < 0.01$. ***$p < 0.001$. ****$p < 0.0001$ versus scrambled control. Data are presented as mean ± SEM.

Supplementary figure 8

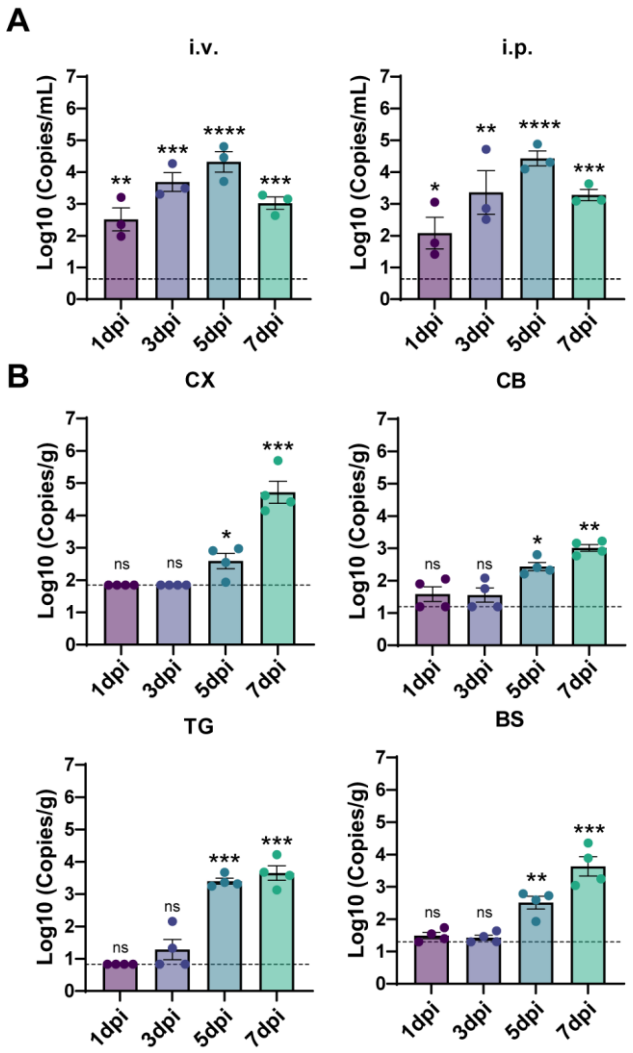

SF 8. DENV-2 infection dynamics in AG129 mice. (A) Viremia levels in AG129 mice inoculated with DENV-2 via the i.v. (left) or i.p. (right) route, quantified by RT-qPCR at 1, 3, 5, and 7 dpi (n=3). (B) Tissue distribution of viral RNA in AG129 mice following i.n. challenge (n=4). CX, cerebral cortex; CB, cerebellum; BS, brainstem; TG, trigeminal ganglion (n=4). * $p < 0.05$, ** $p < 0.01$. ***$p < 0.001$. ****$p < 0.0001$. Data are presented as mean ± SEM.

Supplementary figure 9

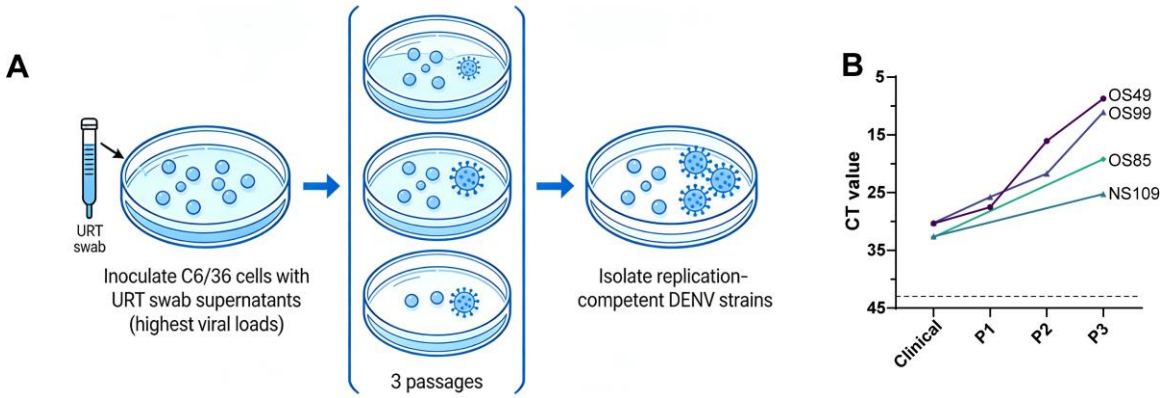

SF 9. Recovery of infectious virus from patient samples in C6/36 cells. (A) Schematic of the experimental timeline for replication-competent virion isolation. (B) Viral RNA levels in the culture supernatant measured by RT-qPCR. Data are presented as mean ± SEM.